Research Paper

Investigation of Characteristics of Decay Parameters Kappa Based on Iranian Dataset

Amir Hossein Shafiee[1], Hamid Zafarani[2*] and Maryam Vajdi Bilesavar[3]

1. Faculty of Civil Engineering and Architecture, Shahid Chamran University of Ahvaz, Ahvaz, Iran
2. Professor, Seismological Research Center, International Institute of Earthquake Engineering and Seismology (IIEES), Tehran, Iran,*Corresponding Author; email: h.zafarani@iiees.ac.ir
3. Research Fellow, International Institute of Earthquake Engineering and Seismology (IIEES), Tehran, Iran

Received: 20/08/2022
Revised: Not Required
Accepted: 07/01/2023

ABSTRACT

The decay parameter κ (Kappa) that was first presented by Anderson and Hough [1] is commonly used to represent the observed decay of acceleration spectrum at high frequencies. It is considered that κ has a direct linear relationship with distance. The intercept of this line is called κ_0, which is a site-dependent component, and it is supposed to be due to attenuation of seismic waves in near-surface layers. Nowadays, these decay parameters have various applications such as estimation of attenuation function in the square-root-impedance method or implementation of host to target method in ground motion prediction equations. However, the characteristics of both κ and κ_0 have not been studied, as it deserves. In the present paper, the decay parameter κ is obtained by the classical approach using 1157 records from all over Iran. The linearity of κ-distance relationship is questioned and investigated for different distances. It is found that the slope of κ-distance relationship reduces significantly at greater distances, and therefore, a linear correlation equation could not predict well enough specially for great distances. Furthermore, the log-likelihood (LLH) criterion is applied to select the best model that correlates κ_0 with V_{S30} for different seismotectonic provinces of Iran. This criterion that is based on the information theory yields that a linear equation can be a better correlation than a rational one. No asymptote value is observed for κ_0 at high values of V_{S30}.

Keywords:
Kappa factor;
Log-likelihood criterion;
Acceleration spectrum;
Strong motion;
Middle-east region

1. Introduction

Anderson and Hough [1] studied the shape of acceleration spectrum of 1971 San Fernando earthquake and 1980 Mexicali valley earthquake at high frequencies. They observed that at frequencies higher than a threshold frequency (f_E), the acceleration spectrum decreases linearly with frequency. Therefore, the function of $a(f)$, versus frequency (f) is as follows:

$$a(f) = A_0 \exp(-\pi\kappa f) \qquad f > f_E \tag{1}$$

where A_0 depends on source properties and epicentral distance, and κ is a decay parameter. Anderson [2] proposed an equation for κ that included a distance-dependent component $\tilde{\kappa}(r)$ and a site-dependent component κ_0, equation (2):

$$\kappa = \kappa_0 + \tilde{\kappa}(r) \tag{2}$$

where r is the epicentral distance, and $\kappa = \kappa_0$ for zero epicentral distance (i.e., κ_0 does not depend on distance). Anderson and Hough [1] concluded that $\tilde{\kappa}(r)$ is due to the horizontal propagation of seismic waves through the crust whereas κ_0 is due to the attenuation of seismic waves through subsurface geological structure. The distance-dependent component $\tilde{\kappa}(r)$ is usually considered to have a linear relation with r (e.g., [3-6]) in the form of equation (3):

$$\kappa = \kappa_0 + m.r \tag{3}$$

where m is the slope and κ_0 is the intercept of the κ vs. r line. However, Anderson and Hough [1] doubted this linear relation, and as mentioned by Anderson [2], the linear relation has no theoretical basis. In another study, Castro et al. [7] investigated the attenuation due to 1976 Fruili earthquake (M6.5) in Italy. They observed a non- linear trend in the κ versus r plot. Even, some studies showed that at high distances κ may be completely independent of distance. Having investigated Guerrero strong motion network in Mexico, Purvance and Anderson [8] assumed a correlation model so that κ varied linearly with distance up to r = 80 km, and then flattened beyond that distance.

The arguments about κ and κ_0 considering their originality and characteristics are still ongoing (see [9] for more details). Ktenidou et al. [10] stated that both material damping and scattering from near-surface layers have contributions to κ_0. Several studies attempted to find a correlation between κ_0 and time-averaged shear wave velocity to a depth of 30 m (V_{S30}). The first correlation probably belonged to Silva et al. [11] who used records form 1989 Loma Prieta earthquake (M6.9) in north California to derive the following equation: log κ_0 = 1.655 - 1.093 log V_{S30}, for $0.004 \le \kappa_0(s) \le 0.068$, and $329 \le V_{S30}$ (m/s) κ 1578. Later, Van Houtte et al. [12] analyzed data from the Japanese KiK-net strong motion network using records between 1998 and 2006 to fit a correlation between natural logarithms of κ_0 (s) and V_{S30} (m/s) as: ln κ_0 = 3.490 - 1.062 ln V_{S30} with a correlation coefficient of 0.39. Having considered the records in Switzerland, Edwards [13] proposed three models for estimation of κ_0 (s) by V_{S30} (m/s) as: (a) $\log \kappa_0 = -1.51 - 0.00031\, V_{S30}$ (called log-lin model, hereafter); (b) $\log \kappa_0 = 0.0854 - 0.653 \log\, V_{S30}$ (called log-log model, hereafter); and (c) $\kappa_0 = 0.274 - 0.0000087\, V_{S30}$ (called lin-lin model, hereafter). The common point of all of the aforementioned relations is that κ_0 decreases with increase of V_{S30}. However, Ktenidou et al. [10] observed that κ_0 first decreases as V_{S30} increases but for values of V_{S30} higher than about 1600 m/s, an asymptote value exists for κ_0. They noted that the value of the asymptote may depend on nature of the crust and regional properties of the rock. They proposed the asymptotic value of $\kappa_0 = 0.021$ s and 0.012 s for northern Greece and Switzerland, respectively. Fu and Li [6] studied attenuation at high frequencies based on 1597 accelerograms from more than 597 events in China. Amazingly, they observed that κ_0 increases with increase of V_{S30}. This observation is unique and has not been reported elsewhere in the literature. They attributed this finding to narrow range of V_{S30} (240 to 600 m/s) in their studied stations. Fu and Li [6] also proposed a linear correlation with decreasing trend between κ_0 and elevation for their studied regions. Some re-searchers attempted to correlate κ_0 with other site-related parameters other than V_{S30}. Campbell [4] mentioned that κ_0 is highly dependent on sediment thickness in eastern North America. He proposed a direct linear relation between κ_0 and sediment thickness that is side dependent. In another study, Van Houtte et al. [12] compared the dependency of κ_0 on V_{S10}, V_{S20}, and V_{S30}. They found that V_{S30} is the best proxy among these three velocities. Ktenidou et al. [10, 14] examined the dependency of κ_0 on resonant frequency and depth to bedrock. They found that these two parameters correlate κ_0 relatively equally well as V_{S30}. Some researches such as Purvance and Anderson [8], Van Houtte et al. [12] and Pavel and Vacareanu [15] also pointed out that source effects may have some influences on κ_0 too.

The decay parameter κ_0 has several applications in seismology such as: (1) determination of site attenuation function in the square-root-impedance method (e.g., [16-18]) and even in the H/V approach (e.g., [3, 19]); (2) contribution in ground motion prediction equations (GMPEs) (e.g., [20-21]) and in host-to-target method where it is used to correct the GMPE for softer grounds (e.g., [22, 24]); and (c) involvement in simulation of ground motion records by stochastic (e.g., [23]) or hybrid methods (e.g., [25-27]).

There are several methods to determine κ and

κ_0 (see [9] for more details). The most important methods probably are: (1) the classic approach that refers to the fundamental definition of κ (Equation 1). Kappa is obtained by computing the slope of Fourier acceleration spectrum above a threshold frequency in a semi-logarithmic plot (e.g., [1]). Multiple subclasses were created for the classic approach such as the one presented by Drouet et al. [28] who used transfer function at $f > 10$ Hz to determine κ_0 directly, or the one applied by Oth et al. [29] who used the Fourier source spectrum at high frequencies; (2) The methods that compute κ_0 by fitting the stochastically generated response spectrum to the observed ones (e.g., [30]); (3) The broadband inversions of entire frequency band for source, path and site effects (e.g., [31]).

A few studies are present in the literature that obtained κ_0 for some regions of Iran. Motazedian [3] and Soghrat et al. [5] determined κ_0 for northern Iran, while Zafarani and Soghrat [19] computed this decay parameter for the Zagros region in Iran using the classic approach for both soil and rock. They obtained $\kappa_0 = 0.0412$ and 0.0184 for soil and rock sites of Zagros, respectively.

This paper, we implemented the classic approach to define κ using a large dataset from Iran. Next, κ_0 is determined for available stations, and the so-called log-likelihood approach is applied to find the best model that correlates κ_0 with V_{S30} for various seismotectonic regions of Iran. During this process, it is attempted to find an answer to the following questions:

- Is a linear relation between κ and *r*, in the form of Equation (3), able to characterize the distance-dependency of κ as it deserves?
- Does the slope of κ versus *r* relation diminish at great distances, as mentioned by Purvance and Anderson [8]
- How is the variation of κ_0 with V_{S30}? Does any asymptotic value exist for κ_0?

2. Dataset and Method of Analysis

2.1. Data

The dataset used for this study consists of 1157 three-component accelerograms recorded at 298 stations with known V_{S30} values all over Iran. The dataset was picked from the large dataset collected by Zafarani and Soghrat [32]. V_{S30}'s have the minimum value of 165 m/s, maximum of 1783 m/s, and mean of 653 m/s. The histogram of V_{S30} is shown in Figure (1).

2.2. Methodology

The Joyner-Boore distance (called *r*, hereafter) of each record is used in the present study. The distance has a minimum value of 0.3 km, maximum of 586.7 km, and mean of 51.9 km. The histogram of this distance is presented in Figure (2).

The classic approach is used to determine κ for each record so that, the slope of Fourier spectrum at high frequencies ($f > 5$ Hz) in a semi-logarithmic plot is computed. κ is obtained by the slope divided by κ (see Equation 1). The vertical component of κ is not considered in the present study. Each record has two horizontal components. As a result, two values of κ are obtained for

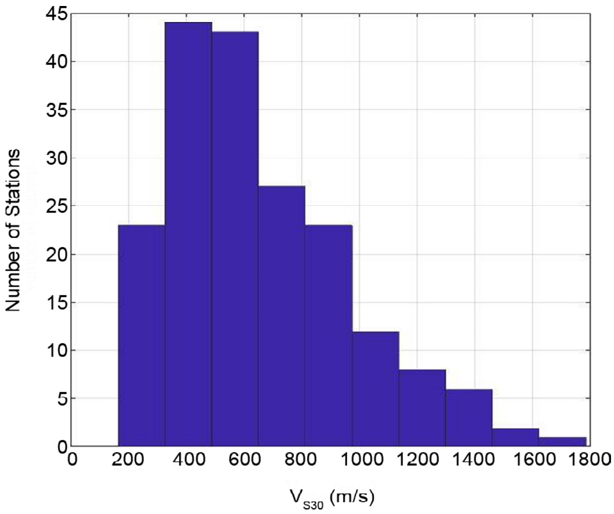

Figure 1. Histogram of V_{S30}.

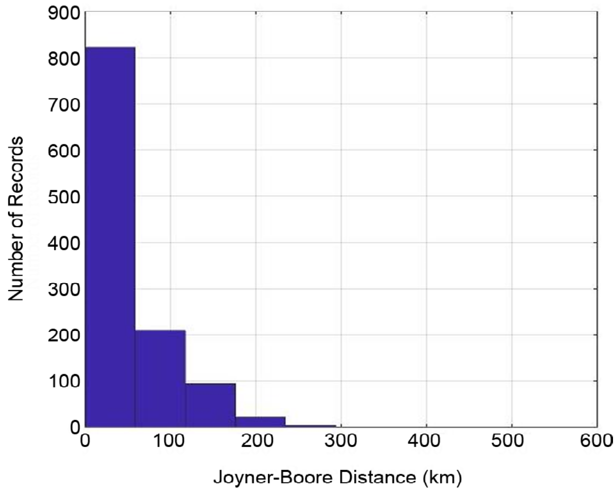

Figure 2. Histogram of Joyner-Boore distance.

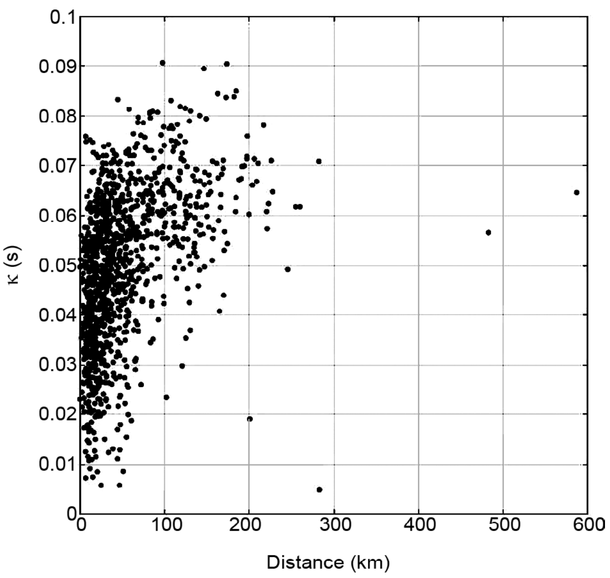

Figure 3. Scatter plot of κ versus *r*.

each record. The average value of these horizontal values is used as the κ value of each record. The scatter plot of κ versus *r* is shown in Figure (3). Then, the least square method is applied to fit a linear relation in the widely-used form of Equation (3). The regression is performed by applying bisquare weights scheme. In this method, smaller weights are assigned to data points further from the model. The resulted fit is:

$$\kappa = 0.04163 + 0.0001638r \tag{4}$$

The fit line of Equation (4) and the corresponding 95% prediction bounds are shown in Figure (4). It is clearly seen that the interval of prediction bounds is wide and the data are very scattered. The R^2 coefficient of Equation (4) is 0.20. Equation (4) also depict that $\kappa_0 = 0.04163$ s for the studied region (i.e. whole Iran). A careful look at Figure (4) raises serious doubts on linearity of κ versus *r* correlation. In order to verify the linearity, we exclude data related to distances lower than 60, 80, and 100 km, at first, and find the linear correlation between κ and *r* for remaining data. The results are shown in Table (1). It is noticed that the slope of the line decreases significantly as *r* increases. This observation reinforces the assumption that κ does not vary linearly with variation of *r*. Therefore, we propose a bilinear fit to the data as:

$$\kappa = \begin{cases} 0.03626 + 0.0003318r, & r < 80 \text{ km} \\ 0.06214 + 0.000008302r, & r \geq 80 \text{ km} \end{cases} \tag{5}$$

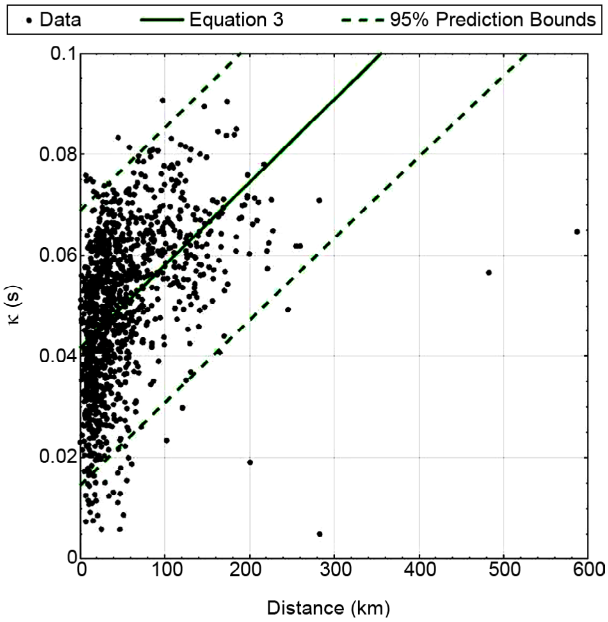

Figure 4. Fit line of Equation (4) and the corresponding 95% prediction bounds.

Table 1. Linear correlation between κ and *r* for various distance ranges

Distance Limitation	Number of Records	Linear Fit: $\kappa = \kappa_0 + m.r$	
		κ_0 (s)	m
$r > 60$ km	327	0.05747	0.00003448
$r > 80$ km	233	0.06214	0.000008302
$r > 100$ km	168	0.06246	0.000006866

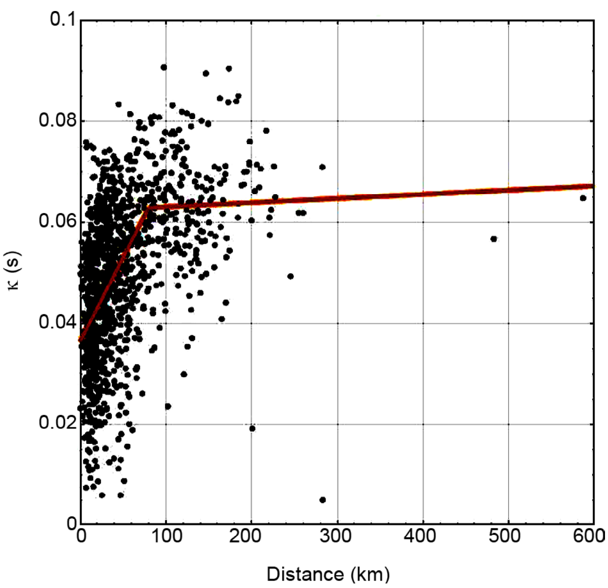

Figure 5. Bilinear correlation of equation (5) and data points.

Based on Equation (5), $\kappa_0 = 0.03626$ for Iran, which is about 13% lower than the one obtained by linear correlation. The bilinear correlation of Equation (5) and the data points are shown in Figure (5). Of course, further analysis using complementary data is required to clarify the nonlinearity of κ versus r correlation.

3. Results

In order to correlate κ_0 and V_{S30}, we separate the data (stations) with more than one record (r value) for a single V_{S30} value at first. 196 V_{S30} values are separated through this process. Then, the intercept of a linear correlation between κ and r (Equation 3) is determined for each of this 196 (r, κ) pairs. This intercept represents κ_0. Consequently, there are 196 V_{S30} values with 196 κ_0 values. It should be mentioned here that 196 V_{S30} values correspond to more than 196 stations since some of the stations have the same V_{S30} values. Seven κ_0's have negative values probably because of lack of enough data for those stations. Remaining κ_0 values have minimum of 0.000299 s, maximum of 1.0031 s, and mean of 0.0565 s. The scatter plot of (κ_0, V_{S30}) pairs is shown in Figure (6). The upper limit of Y-axis is assigned to 0.2 to show the scattering of data better (there are just four κ_0's higher than 0.2). Using nonlinear least-squares regression with bisquare weight, we propose the following correlation for Iran:

$$\kappa_0 = 0.05774 - 0.0000215\, V_{S30} \tag{6}$$

with $R^2 = 0.93$. It is seen that the increase of V_{S30} results in decrease of κ_0. The same trend exists in relations of Silva et al. [30], Van Houtte et al. [12], and Edwards [13] too (see the Introduction section). However, Ktenidou et al. [10] mentioned that κ_0 may have an asymptotic value at high values of V_{S30}. In order to examine this claim, we select a fit with asymptote in a rational form using the same method of regression. The fit equation is:

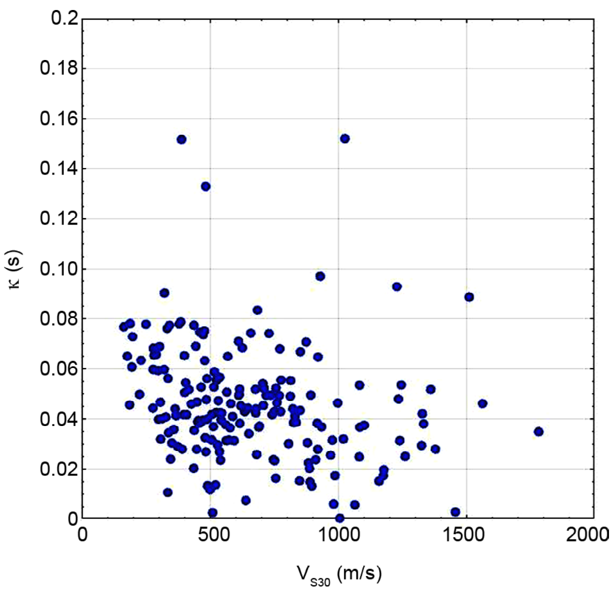

Figure 6. Scatter plot of κ_0 versus V_{S30}.

$$\kappa_0 = \frac{0.02811 V_{S30} + 10.4}{V_{S30} + 48.39} \tag{7}$$

Equation (6) has the minimum of $\kappa_{0\min} = 0.02811\,\mathrm{s}$ as an asymptote. The log-likelihood (LLH) criterion, which is based on the information theory is implemented to select the best model. This method also assigns weight factors to each model to use in a logic-tree approach. The LLH of a model with samples x_1 through x_N is determined by (Scherbaum et al. [33]):

$$LLH = -\frac{1}{N}\sum_{i=1}^{N}\log_2\left[g\left(x_i\right)\right] \tag{8}$$

where N is the number of samples, and $g(x)$ represents the probability distribution function of the model. The better model has the smaller value of LLH (i.e., less information is lost when the real data is replaced by model). This approach assigns a weight factor (w_i) to each candidate model as:

$$w_i = \frac{2^{-LLH(g_i,x)}}{\sum_{j=1}^{K} 2^{-LLH(g_j,x)}} \tag{9}$$

where K is the total number of models. Mousavi et al. [34] and Shafiee et al. [35] applied this criterion to different seismological issues related to Iran.

Having applied the *LLH* criterion to the linear model (Equation 6) and the rational model (Equation 7), the *LLH* values of the linear model and the rational model are -5.029 and -5.173, and the weight factors are 0.475 and 0.525, respectively. Therefore, the rational model is the best model. In other words, the existence of an asymptote value of κ_0 equal to 0.02811 s could be valid for our data. However, the difference between the weight factors is small. We propose to use both models in a logic-tree approach as:

$$\kappa_0 = 0.475\kappa_{0(Eq.6)} + 0.525\kappa_{0(Eq.7)} \tag{10}$$

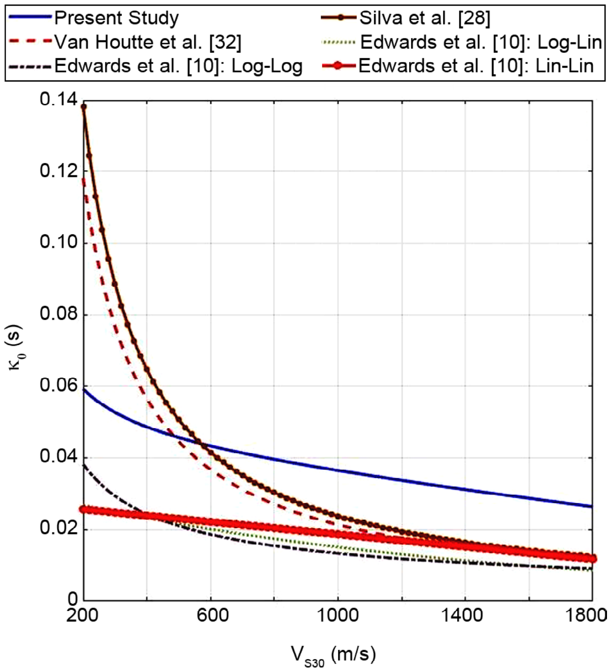

Figure 7. Comparison of the model of the presented study with the models previously published in the literature.

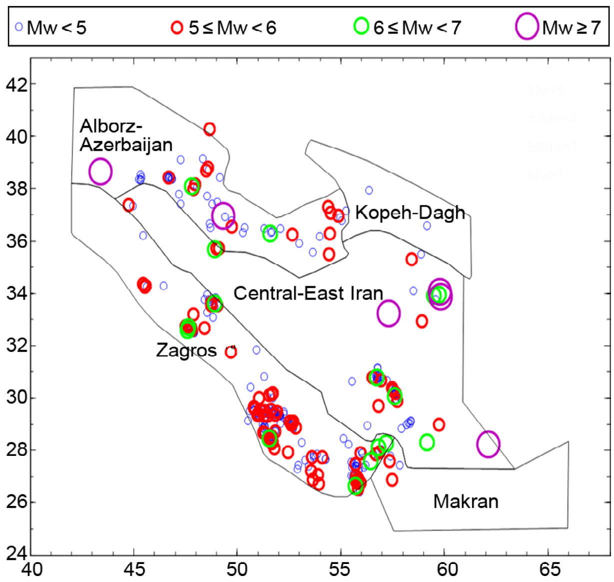

Figure 8. Major Seismotectonic regions of Iran [36].

for Iran, where $\kappa_{0(Eq.6)}$ and $\kappa_{0(Eq.7)}$ are κ_0's obtained by Equations (6) and (7), respectively. The comparison of the presented study with other correlations presented in the literature is clearly shown in Figure (7). It is observed that for V_{S30} values lower than about 485 m/s, the κ_0's of the present study is lower than those of Silva et al. [30] and Van Houtte et al. [15] and higher than all of the Edwards et al. [13] models, while for higher values of V_{S30} (higher than about 568 m/s) the results of the present study are the highest curves.

Iran is a large country including various seismotectonic and geologic units. Mirzaei et al. [36] divided Iran to five seismotectonic regions as: Azerbaijan-Alborz, Central-East, Zagros, Kopeh Dagh, and Makran as shown in Figure (8). We use the regions presented by Mirzaei et al. [36] to fit κ_0 versus V_{S30} correlation for each of the aforementioned regions. 74 (κ_0, V_{S30}) pairs lied in the Azerbaijan-Alborz region, 47 in Central-East, 73 in Zagros, 3 in Kopeh Dagh, and 4 in Makran. Both linear and rational forms of correlations are fitted to each region except Kopeh Dagh and Makran that are excluded because of lack of enough data at these two regions. Then, the *LLH* criterion is applied to each model and the weight factor is determined for each of them.

The results are shown in Table (2). It is observed that the rational model is a better fit for Azerbaijan-Alborz region whereas both models fit almost equally well for Central-East region and the linear model is a little better correlation for Zagros region. We used the computed weight factors in a manner similar to Equation (10) to determine κ_0 for each region. The final results are shown in Figure (9). It is noticed that the Azerbaijan-Alborz region has the highest κ_0 for V_{S30} values up to about 600 m/s, whereas the Central-East region is on top for higher values of V_{S30}. Moreover, the κ_0 values for Zagros region is minimum for V_{S30}'s lower than about 880 m/s, while the Azerbaijan-Alborz

Table 2. The results of the application of the LLH criterion to both linear and rational fits.

Regions	Linear: $\kappa_0 = a - b.V_{S30}$		Rational: $\kappa_0 = \frac{p.V_{S30}+q}{V_{S30}+r}$			LLH		Weight Factor	
	a	***b***	***p***	***q***	***r***	**Linear**	**Rational**	**Linear**	**Rational**
Azerbaijan-Alborz	0.06406	0.00003005	0.01931	23.49	219.1	-4.5227	-4.7931	0.453	0.547
Central-East Iran	0.05346	0.00001357	0.03666	1.369	-58.45	-5.9030	-5.9040	0.500	0.500
Zagros	0.04526	0.000008968	0.01702	70.04	1420	-6.4076	-6.3888	0.503	0.497

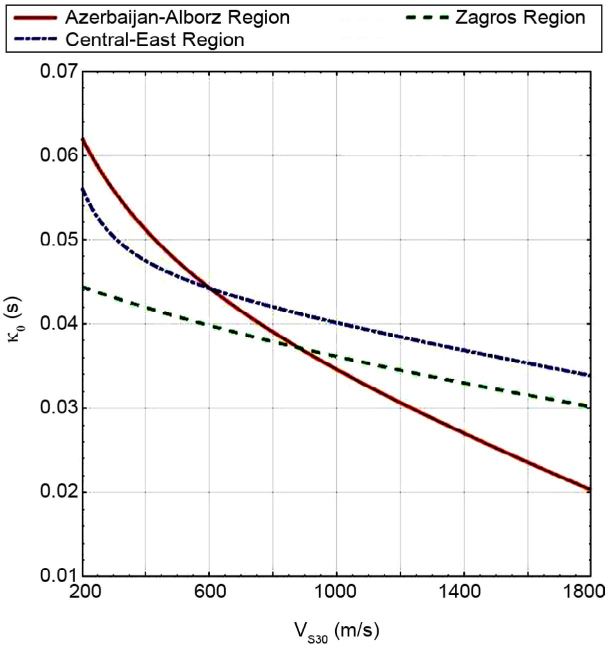

Figure 9. Variations of κ_0 versus V_{S30} for Azerbaijan-Alborz, Central-East Iran, and Zagros regions.

region owns the minimum values at higher values of V_{S30}.

4. Discussion and Conclusions

Rigorous statistical analyses were carried out to determine characteristics and variations of decay parameter Kappa using dataset from Iran. The dataset consists of 1157 κ values obtained by the classic approach. At first, the dependency of κ to distance (r) was investigated. Having fitted a line to (κ, r) pairs using the least-squares method, the value of intercept (κ_0) was obtained to be equal to 0.04163 s for the study area. Although the linearity of κ and r relation is widely considered and accepted in the literature, it was observed that κ values fell off at high distances. The authors proposed a bilinear relationship to represent this behavior.

In the next step, it was attempted to find a correlation between κ_0 and V_{S30} not just for Iran as an entire unit, but also for various seismotectonic regions of the country. Two kinds of models were considered: a linear model, and a rational one. The rational model represented a model with an asymptotic value. The *LLH* criterion was implemented to select the best model. This criterion is based on the information theory and takes into account the amount of information loss through modeling the real data. The results of the analyses showed that the rational model is the best fit for entire Iran and the Azerbaijan-Alborz region (i.e., it has smaller value of *LLH* with respect to the rational model). Hence, the acclaim of existence of a minimum κ_0 value, corresponding to an asymptotic line, was observed in the present study. The *LLH* approach has the advantage of assigning weight factor to each model. As a result, all models can be used in a logic-tree approach by using these weight factors. Thus, none of the models are indeed excluded. The present correlation was also compared with those available in the literature. It was noticed that the present correlation gave the maximum κ_0 values for V_{S30}'s higher than about 568 m/s. Furthermore, the comparison of correlation curves of various regions of Iran showed that for V_{S30}'s higher than about 880 m/s, the Central-East region curve lied on top, while the curve corresponding to the Azerbaijan-Alborz region is on bottom.

The results of the present study can be used in derivation of GMPE's for Iran using host-to-target approach by Campbell [22] or determination of attenuation function in the square-root-impedance method by Boore and Joyner [16].

Acknowledgements

The authors acknowledge the Building and Housing Research Centre of Iran for providing them with the accelerograms and shear-wave velocities used in the current study. They also thank the continuing support of the International Institute of Earthquake Engineering and Seismology during this research.

References

1. Anderson, J.G. and Hough, S.E. (1984) A model for the shape of the Fourier spectrum of acceleration at high frequencies. *Bull. Seismol. Soc. Am.*, **74**, 1969-1993.

2. Anderson, J.G. (1991) A preliminary descriptive model for the distance dependence of the spectral decay parameter in southern California. *Bull. Seismol. Soc. Am.*, **81**, 2186-2193.

3. Motazedian, D. (2006) Region-specific key seismic parameters for earthquakes in Northern Iran. *Bull. Seismol. Soc. Am.*, **96**, 1383-1395.

4. Campbell, K.W. (2009) Estimates of shear-wave Q and κ_0 for unconsolidated and semiconsolidated sediments in Eastern North America. *Bull. Seismol. Soc. Am.*, **99**, 2365 2392.

5. Soghrat, M.R., Khaji, N., and Zafarani, H. (2012) Simulation of strong ground motion in northern Iran using the specific barrier model. *Geophys. J. Int.*, **188**, 645-679.

6. Fu, L. and Li, X. (2016) The Characteristics of high-frequency attenuation of shear waves in the Longmen Shan and adjacent regions. *Bull. Seismol. Soc. Am.*, **106**(5), 1979-1990.

7. Castro, R., Pacor, F., Sala, A., and Petrungaro, C. (1996) S wave attenuation and site effects in the region of Friuli, Italy. *J. Geophys. Res.*, **101**, 22355-22369.

8. Purvance, M.D. and Anderson J.G. (2003) A comprehensive study of the observed spectral decay in strong-motion accelerations recorded in Guerrero, Mexico. *Bull. Seismol. Soc. Am.*, **93**, 600-611.

9. Ktenidou, O.J., Cotton, F., Abrahamson, N.A., and Anderson, J.G. (2014) Taxonomy of κ: A review of definitions and estimation approaches targeted to applications. *Seismol. Res. Lett.*, **85**, 135-146.

10. Ktenidou, O.J., Abrahamson, N.A., Drouet, S., and Cotton F. (2015) Understanding the physics of kappa (κ): Insights from a downhole array. *Geophys. J. Int.*, **203**, 678-691.

11. Silva, W., Darragh, R., Gregor, N., Martin, G., Abrahamson, N., and Kircher, C. (1999). *Reassessment of Site Coefficients and Near-Fault Factors or Building Code Provisions*. Tech. Rept. Program Element II: 98-HQ-GR-1010, Pacific Engineering and Analysis, El Cerrito, California.

12. Van Houtte, C., Drouet, S., and Cotton, F. (2011) Analysis of the origins of κ (kappa) to compute hard rock to rock adjustment factors for GMPEs. *Bull. Seismol. Soc. Am.*, **101**, 2926 2941.

13. Edwards, B. (2012) *Site Specific Kappa, Technical Report SED/PRP/R/035b/20120410*, Swiss seismological service, Zurich, Switzerland.

14. Ktenidou, O.J., Cotton, F., Chaljub, E., Drouet, S., Theodoulidis, N., and Arnaouti S. (2012) Estimation of kappa (κ) for a sedimentary basin in Greece (EUROSEISTEST) - correlation to site. *Proc. 15th World Conf. on Earthquake Engineering*, Lisbon.

15. Pavel, F. and R., Vacareanu (2015) Kappa and regional attenuation for Vrancea (Romania) earthquakes. *J. Seismol.*, **19**, 791-799.

16. Boore, D.M. and Joyner, W.B. (1997) Site amplifications for generic rock sites. *Bull. Seismol. Soc. Am.*, **87**, 327-341.

17. Huang, M.W., Wang, J.H., Ma, K.F., Wang, C.Y., Hung, J.H., and Wen, K.L. (2007) Frequency-dependent site amplifications with $f \geq 0.01$ Hz evaluated from velocity and density models in Central Taiwan. *Bull. Seismol. Soc. Am.*, **97**, 624-637.

18. Jahanandish, M., Zafarani, H., and Shafiee, A.H. (2016) Implementation of the square-root-impedance method to estimate site amplification in Iran using random profile generation. *Bull. Seismol. Soc. Am.*, **107**, 456-467.

19. Zafarani, H. and Soghrat, M. (2012) Simulation of ground motion in the Zagros region of Iran using the specific barrier model and the stochastic method. *Bull. Seismol. Soc. Am.*, **102**, 2031 2045.

20. Toro, G.R., Abrahamson, N.A., and Schneider, J.F. (1997) Model of strong ground motions from earthquakes in central and eastern North America: Best estimates and uncertainties. *Seismol. Res. Lett.*, **68**, 41-57.

21. Atkinson, G.M. and Boore, D.M. (2006) Earthquake ground-motion prediction equations for eastern North America. *Bull. Seismol. Soc. Am.*, **96**, 2181-2205.

22. Campbell, K.W. (2003) Prediction of strong ground motion using the hybrid empirical method and its use in the development of ground motion (attenuation) relations in eastern North America. *Bull. Seismol. Soc. Am.*, **93**, 1012-1033.

23. Zafarani, H., Noorzad, A., Ansari, A., and Bargi, K. (2009) Stochastic modeling of Iranian earthquakes and estimation of ground motion for future earthquakes in Greater Tehran. *Soil Dynam. Earthq. Eng.*, **29**, 722-741.

24. Cotton, F., Scherbaum, F., Bommer, J.J., and Bungum, H. (2006) Criteria for selecting and adjusting ground-motion models for specific target regions: Application to central Europe and rock sites. *J. Seismol.*, **10**, 137-156.

25. Mai, P.M., Imperatori, W., and Olsen, K.B. (2010) Hybrid broadband groundmotion simulations: combining long-period deterministic synthetics with high-frequency multiple S-to-S backscattering. *Bull. Seismol. Soc. Am.*, **100**(5), 2124-2142.

26. Vahidifard, H., Zafarani, H., and Sabbagh-Yazdi, S.R. (2017) Hybrid broadband simulation of strong-motion records from the September 16, 1978, Tabas, Iran, earthquake (Mw 7.4). *Natural Hazards*, **87**, 57-81.

27. Pezeshk, S., Zandieh, A., Campbell, K.W., and Tavakoli, B. (2018) Ground-motion prediction equations for central and eastern North America using the hybrid empirical method and NGA-West2 empirical ground-motion models. *Bull. Seismol. Soc. Am.*, **108**, 2278-2304.

28. Drouet, S., Cotton, F., and Guéguen, P. (2010) V_{S30}, κ, regional attenuation and Mw from small magnitude events accelerograms. *Geophys. J. Int.*, **182**, 880-898.

29. Oth, A., Bindi, D., Parolai, S., and Giacomo, D.D. (2011) Spectral analysis of K-NET and KiK-net data in Japan, Part II: On attenuation characteristics, source spectra, and site response of borehole and surface stations. *Bull. Seismol. Soc. Am.*, **101**, 667-687.

30. Silva, W.J. and Darragh, R. (1995). *Engineering Characterization of Earthquake Strong Ground Motion Recorded at Rock Sites*. Palo Alto, Electric Power Research Institute, TR-102261.

31. Edwards, B., Faeh, D., and Giardini, D. (2011) Attenuation of seismic shear wave energy in Switzerland. *Geophys. J. Int.*, **185**, 967-984.

32. Zafarani, H. and Soghrat, M. (2017) A selected dataset of the Iranian strong motion records. *Natural Hazards*, **86**, 1307-1332.

33. Scherbaum, F., Delavaud, E., and Riggelsen, C. (2009) Model selection in seismic hazard analysis: An information-theoretic perspective. *Bull. Seismol. Soc. Am.*, **99**, 3234-3247.

34. Mousavi, M., Zafarani, H., Rahpeyma, S., and Azarbakht, A. (2014) Test of goodness of the NGA ground-motion equations to predict the strong motions of the 2012 Ahar-Varzaghan dual earthquakes in northwestern Iran. *Bull. Seismol. Soc. Am.*, **104**, 2512-2528.

35. Shafiee, A.H., Zafarani, H., and Jahanandish, M. (2016) Model selection for correlating V_{S30} with average shear-wave velocities at lower depths based on the Iranian data. *Bull. Seismol. Soc. Am.*, **106**, 289-299.

36. Mirzaei, N., Mengtan, G., and Yuntai, C. (1998) Seismic source regionalization for seismic zoning of Iran: major seismotectonic provinces. *J. Earthq. Pred. Res.*, **7**, 465-495.